Longitudinal Phase Space Evolution and Tomographic Reconstruction at FACET

S. Gessner, E. Adli, C.I. Clarke, S. Corde, F.J. Decker, A.S. Fisher, J. Frederico,
M.J. Hogan, N. Lipkowitz, S. Li, M. Litos, D. Walz, G. White, V. Yakimenko, and G. Yocky

SLAC National Accelerator Laboratory, Menlo Park, CA 94025, USA

(Dated: February 16, 2014)

The Facility for Advanced Accelerator Experimental Tests (FACET) at SLAC produces high energy electron beams for Plasma Wakefield Acceleration (PWFA). PWFA experiments require high charge, high peak-current bunches in order to drive large amplitude wakes in the plasma. Creating short bunches with high charge requires detailed knowledge and control of the longitudinal phase space as it evolves in the linac. In this paper, we provide an overview of the bunch compression scheme at FACET and describe a novel tomographic method that allows us reconstruct the beam's longitudinal phase space at the end of the linac.

I. INTRODUCTION

The Facility for Advanced Accelerator Experimental Tests (FACET) at SLAC produces high energy electron beams for Plasma Wakefield Acceleration (PWFA) [1]. PWFA experiments require high charge, high peak-current bunches in order to drive large amplitude wakes in the plasma. Creating short bunches with high charge requires detailed knowledge and control of the longitudinal phase space as it evolves in the linac. In this paper, we provide a detailed description of the bunch compression scheme at FACET and describe a novel diagnostic for reconstructing the longitudinal phase space at the end of the linac.

FACET combines RF and wakefield chirping mechanisms with bunch compressor chicanes to generate the shortest bunches possible.

The 2D longitudinal particle tracking code LiTrack is used to supplement our understanding of the phase space in regions of the linac where diagnostics are not available.

The final bunch length is sensitive to many parameters in the linac, including initial bunch length, RF chirp phase, and the R_{56} of compressor chicanes. To the greatest extent possible, feedbacks are implemented to control and stabilize the beam as it evolves in the linac. Some parameters are not under feedback control, and for this reason it is critical to have real time diagnostics for the bunch length, energy spectrum, and longitudinal phase space.

FACET uses an x-band transverse deflecting cavity (TCAV) for precision bunch length measurements and a half-period wiggler magnet for non-destructive energy spectrum measurements. These two diagnostics provide projections of the longitudinal phase space. A third measurement was developed by creating a tunable momentum aperture, or slit, and using the TCAV and spectrometer to diagnose mono-energetic slices of the beam. By combining the bunch profiles measured for each slice, we were able to tomographically reconstruct the beam's longitudinal phase space. The longitudinal phase space uniquely encodes the longitudinal evolution of the beam in the linac. This technique allows us to determine errors in linac parameters and is a valuable tool for beam tuning.

II. LONGITUDINAL PHASE SPACE EVOLUTION

The FACET linac is 2 kilometers long and accelerates a 3.2 nC electron beam to 20.35 GeV. The beam is generated from a thermionic cathode at the west end of the linac and captured by the Sector 0 RF cavities. It is accelerated to 1.19 GeV in the Sector 1 s-band cavities and is transferred to the North Damping Ring (NDR) via the North Linac to Ring chicane (NLTR). The beam is transversely and longitudinally damped in the NDR before it is extracted into the North Ring to Linac chicane (NRTL). The NRTL is the first of three bunch compressor chicanes at FACET. The beam is accelerated to 9 GeV and chirped by the RF in the first kilometer of the linac (Sectors 2-10) before being compressed again in the Sector 10 chicane. Following the Sector 10 chicane, the beam is accelerated on crest to 20.35 GeV in the second kilometer of the linac (Sectors 11-19). Beam induced wakefields provide a chirp in this portion of the beamline before the bunch undergoes final compression in the FACET W-chicane. Figure 1 shows the beamline elements that effect the longitudinal evolution of the beam.

A. North Damping Ring

The longitudinal bunch parameters prior to injection in the NDR are approximately $\sigma_z = 2.33$ mm and $\delta = 1\%$ which gives a longitudinal phase space volume of $\varepsilon_0 = \sigma_z \sigma_\delta = 27.73$ MeV·mm. Once the beam is in the ring, the bunch is radiatively damped to an equilibrium bunch length and an equilibrium energy spread. The bunch is stored in the ring for 16.7 ms and the longitudinal damping time $\tau_z = 1.79$ ms.

Another benefit the radiation damping mechanism is that it provides a useful bunch length diagnostic early in the machine. We imaged synchrotron radiation generated by the beam in one of the bends with a Hama-
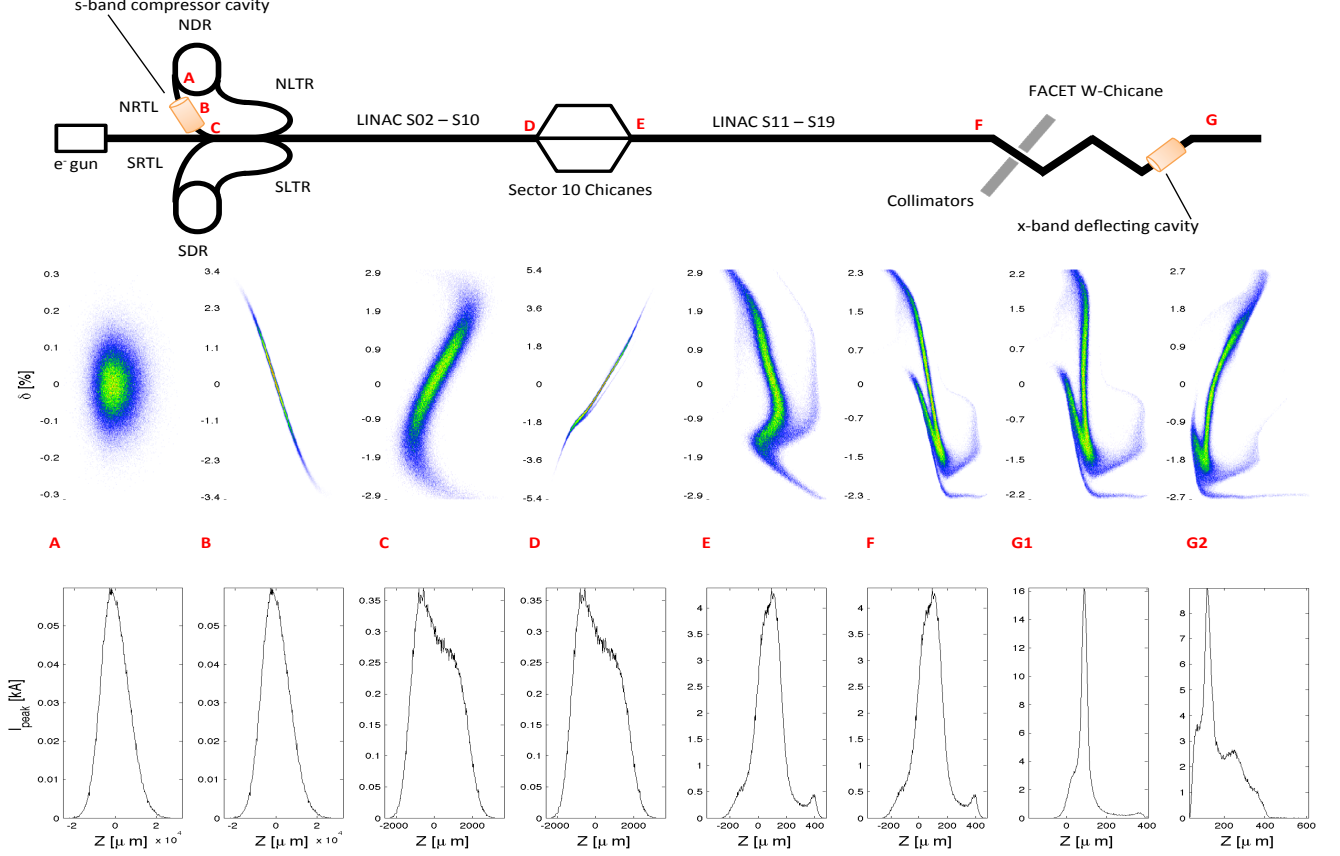
FIG. 1. Overview of the FACET Linac.

matsu C5680 streak camera. The camera was operated in "synchroscan" mode, so that the bunch profile can be measured for multiple passes of the beam during the store. Figure 2 shows the streaked beam image for the final fives turns before extraction. The bunch is fit to an asymmetric gaussian with the form

$$\lambda(z) = \frac{N_b}{\sqrt{2\pi}\sigma_z} \exp\left[-\frac{1}{2}\left(\frac{z}{(1 \pm A)\sigma_z}\right)^2\right]. \qquad (1)$$

$z = ct - s$ is the co-moving beam coordinate with the head of the beam at $z < 0$. N_b is the number of beam electrons and A is the asymmetry factor. The asymmetry arrises from the distortion of the RF potential due to beam loading. The measured bunch length was $\sigma_z = 6.59$ mm, about 20% longer than what was measured during SLC operation for similar bunch charge and RF parameters [2].

The equilibrium energy spread was measured to be $\sigma_\delta = 8.11 \times 10^{-4}$. There is no time-energy correlation in the beam after it has been damped, so the longitudinal phase space volume out of the ring is $\varepsilon_{NDR} = 5.57$ MeV·mm. ε_{NDR} sets a lower limit on the final bunch length that can be achieved at the end of the linac.

B. Chirping and Compression in the First Half of the Linac

The FACET linac uses more than 500 constant gradient RF cavities to accelerate the beam to its final energy. The energy gain of a particle in an RF cavity is given by

$$W_{RF}(z) = eEL\cos(kz + \phi) \qquad (2)$$

for cavity field strength E, cavity length L, RF wavenumber k, and cavity phase ϕ. Cavity phase is defined such that 0° is on crest and negative phases are ahead of crest, consistent with the definition of z given in Section II A. The accelerating sections can also be used to chirp the beam. We define the chirp from an accelerating section as the derivative of the energy gain evaluated at the center of the bunch, multiplied by the length of the bunch

$$C_{RF} = \sigma_z \left.\frac{dW_{RF}}{dz}\right|_{z=0} = -\sigma_z eELk\sin\phi. \qquad (3)$$

The chirp is positive if the energy of the beam particles increases with z. This is a useful definition of chirp because it can be applied to both RF phase chirping and the longitudinal wakefield chirping described in Section II C.
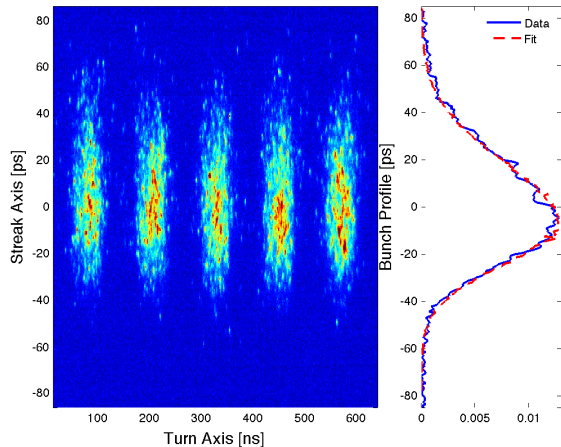
FIG. 2. Streak camera image of the final five turns before extraction from NDR. The bunch profile on the right is the average of the five turns shown, fit to an asymmetric gaussian with $\sigma_t = 22$ ps or $\sigma_z = 6.59$ mm, and asymmetry parameter -0.2.

The first RF cavity encountered by the electron beam after extraction from the NDR is the s-band compressor in the North Ring to Linac (NRTL) chicane. The compressor cavity is operated at the 90° zero-crossing so that the beam is maximally chirped.

The beam is compressed by a factor of 10 in the North Ring to Linac (NRTL) chicane and enters the Linac with a 600 μm RMS bunch length. The bunch is slightly over-compressed, with a residual low-to-high chirp, so as to minimize the impact of wakefields in the linac. The bunch is accelerated in the first kilometer of the linac with a net phase of -20 degrees with respect to the crest (in SLAC coordinates, negative angles are ahead of crest). FACET uses a unique chirping scheme in the front end of the linac that staggers the phasing of the beam over nine linac sectors. The staggered chirp process is depicted in Figure 3. By accelerating on crest or nearly on crest in the first few sectors, the beam becomes stiff and more resistant to emittance dilution from transverse wakefields. The later sectors have stronger phasing, up to -55 degrees off crest, in order to achieve an average of -20 degrees chirp prior to the Sector 10 Chicane. While this scheme has the advantage of reducing emittance growth, it makes the beam more sensitive to phase errors in the highly chirped sectors.

The bunch is compressed by another factor of 10 in the Sector 10 Chicane.

C. Wakefield Chirping and Compression in the W-Chicane

Again, the bunch is over-compressed, this time with a residual high-to-low chirp. The very short (50 μm), very high charge (3.2 nC) bunch drives a high-amplitude

longitudinal wakefield in the SLAC s-band cavities. The wakeloss function $W(z)$ is a convolution of the cavity wake structure and the bunch profile, but for very short bunches it is roughly linear over the core of the bunch. The net effect of the wakefields in the second kilometer of the linac is to provide a mostly linear high-to-low chirp that will be leveraged for bunch compression in the FACET W-Chicane.

The FACET W-Chicane is a unique lattice that features adjustable R_{56}. When extremely short bunches are needed, the chicane is tuned to $R_{56} = 5$ mm and yields a gaussian bunch with $\sigma_z = 20$ μm. For the two-bunch setup, the $R_{56} = 10$ mm, which over-compresses the bunch with a residual low-to-high chirp. Table I lists

Element	R_{56} [mm]	ϕ_{rf}	σ_z [μm]
NDR			6600
NRTL Cavity		90°	6600
NRTL Chicane	602.6		500
S02-10		-20°	500
S10 Chicane	-75.8		50
S11-19		0°	50
W-Chicane	5,10		20,200

TABLE I. Table of linac parameters and bunch lengths for each linac element. We quote the two R_{56} values typically used in the W-Chicane.

III. DIAGNOSTICS

A transverse deflecting x-band cavity (TCAV) is located near the end of the W-Chicane, close to maxima in β_y. The TCAV is used as a vertical streaking device; electrons with different longitudinal positions z in
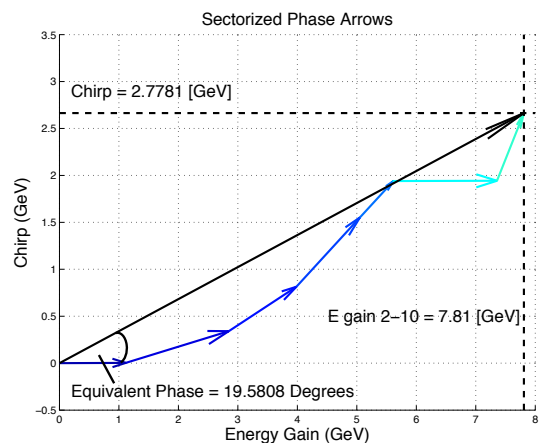

FIG. 3. Diagram showing the phasing in sectors 2-10 at FACET. Each arrow represents the phase and amplitude of the accelerating sector. Note that the chirping angle is depicted as a positive value for clarity.

a bunch experience different transverse deflecting fields. The particles are displaced vertically according to

$$\Delta Y = R_{34} \frac{eV_{rf}}{E_0} \sin kz \qquad (4)$$

and R_{34} is the matrix element between the TCAV and the location where the streaked beam is imaged on a screen. The TCAV phase is calibrated such that the position $z = 0$ in the beam corresponds to the zero crossing of the deflecting wave. The TCAV is the only diagnostic that has been used experimentally to resolve femtosecond beam structures. However, the TCAV is a destructive diagnostic, so it is not used while taking experimental data with plasma.

A half-period wiggler magnet is located just downstream of the TCAV at a dispersive point with the same η and β as the notch collimator. The wiggler deflects the horizontally-dispersed beam vertically. This generates a streak of synchrotron x-rays which are intercepted by a scintillating YAG:Ce crystal millimeters above the beam path. The x-ray streak encodes the energy spectrum of the beam onto the crystal, which is imaged by a CCD camera. On average, each 20.35 GeV electron radiates away 67 KeV of x-rays Emittance dilution due to ISR and CSR is negligible, so we the wiggler/YAG energy spectrometer is non-destructive. This is a particularly useful diagnostic, because it provides information about the longitudinal phase space on every shot.

IV. TOMOGRAPHIC PHASE SPACE RECONSTRUCTION

An ideal phase space measurement allows for the entire beam phase space to be imaged in a single shot. For instance, the LCLS TCAV streaks the beam horizontally before the beam passes through a vertical dipole, so that $Z \rightarrow X$ and $\delta \rightarrow Y$. The beam is imaged on a screen at a point of large R_{15} and large R_{36}. Using this method, the longitudinal phase space is determined for every shot.

At FACET, it is not possible to streak and disperse the beam in orthogonal planes without significant changes to the chicane and final focus optics. Instead, we have developed a technique that allows us to tomographically reconstruct the beam's longitudinal phase space. We use the jaw collimators at the beginning of the FACET chicane to create a narrow slit and use the TCAV to streak the portion of the beam that passes through the slit. The collimators are located in a region with good dispersive contrast, where the ratio $\eta\delta/\sqrt{\beta\varepsilon}$ is at a maximum, so the slit acts as a momentum aperture. The collimators are scanned across the path of the dispersed beam while maintaining a constant slit width of roughly 180 μm or $\Delta E/E = 0.25\%$. The longitudinal bunch profile is recorded for each position of the slit and each profile represents the z-distribution of the bunch at a given δ. Figure 4 shows the measured energy spectrum of the beam

with the collimators open and with the slit in place and Figure 5 shows the same shots measured by the TCAV.
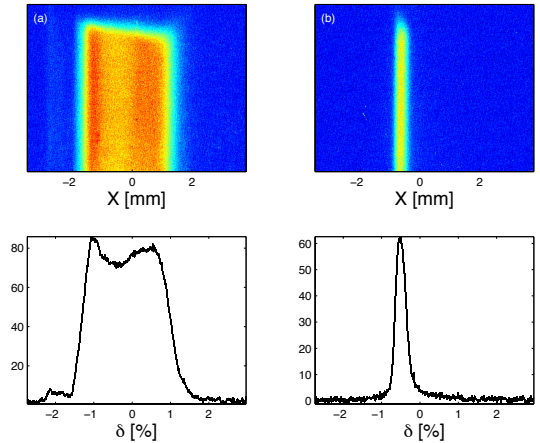

FIG. 4. (a) The full beam energy spectrum imaged at the wiggler spectrometer. (b) The partial energy spectrum with the slit acting as a momentum aperture. The dispersion was measured to be 128 mm at this location.
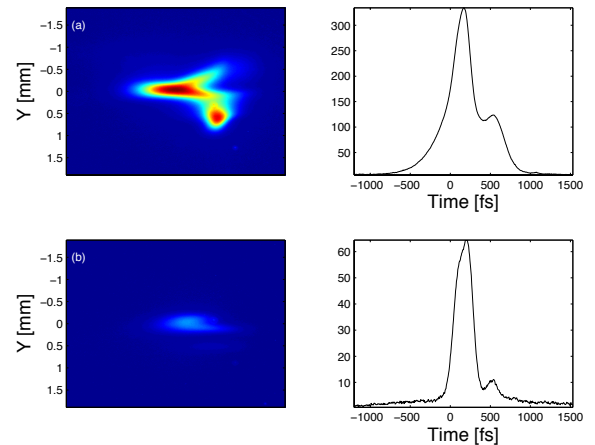

FIG. 5. (a) The full bunch profile as measured with the TCAV. (b) The bunch profile measured for a monoenergetic beam slice.

There is an arrival time jitter of the beam relative to the RF phase of the TCAV. The shots in this dataset have an RMS jitter of 124 fs. By taking multiple shots per slit position, we can find an average temporal position of the profiles. Each set of 20 shots is aligned to the average position. The profiles for each slit position are stacked together to reconstruct the longitudinal phase space. Figure 6 shows the raw data from a measurement taken for 10 slit positions with 20 shots each
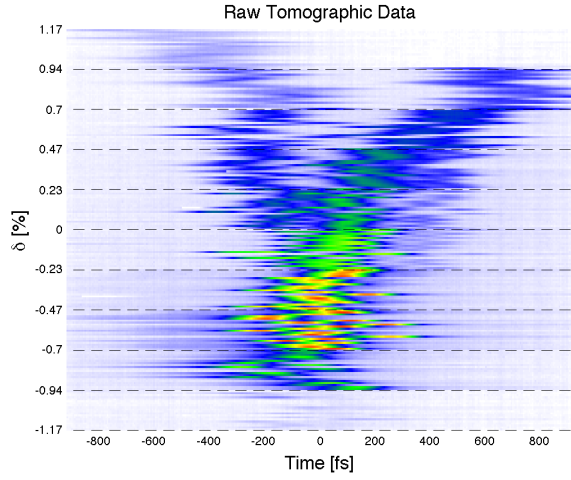
FIG. 6. Raw data from the tomographic slit scan measurement. Note that the δ axis is not continuous. The dashed black lines denote consecutive shots for each slit position.
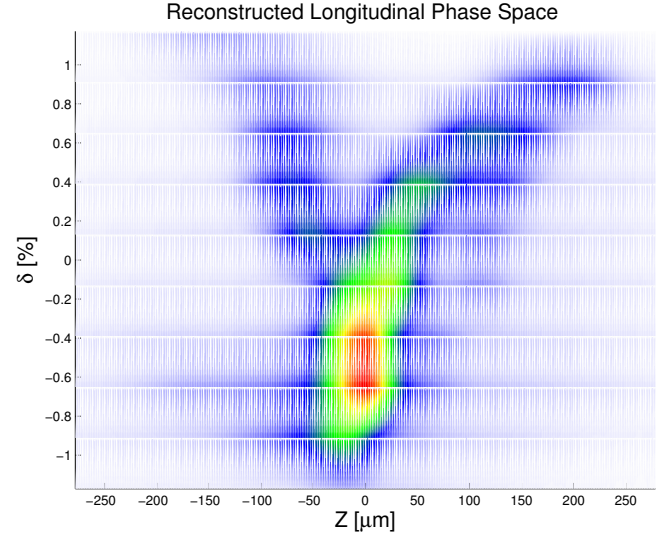

FIG. 7. Raw data from the tomographic slit scan measurement.

V.   CONCLUSIONS AND FUTURE WORK

xxxxxxxxxx

[1] M. J. Hogan et al., New J. Phys. 12, 055030 (2010).
[2] R. Holtzapple, Ph.D. Thesis, Stanford University (1996).